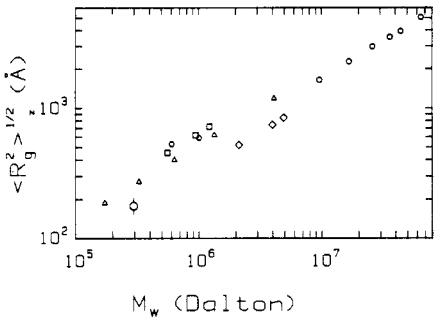

Figure 13. log–log plot of R_g versus M_w for different polymer solutions (same as Figure 9 of ref 10): Δ and ○, polystyrene in benzene; ◇, polymethyl methacrylate in methyl methacrylate; ○, polyethylene in 1,2,4-trichlorobenzene; □, PETFE in diisobutyl adipate; ◇, PTFE in oligomers of poly(chlorotrifluoroethylene).

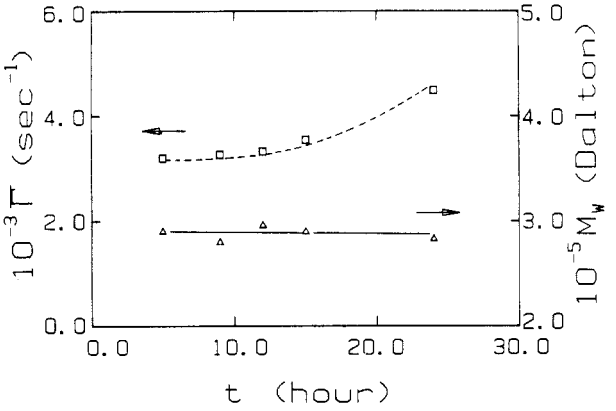

Figure 14. Stability of PTFE solution at 340 °C in terms of M_w and $\bar{\Gamma}$: triangles, M_w; squares, $\bar{\Gamma}$ at $\theta = 30°$.

Teflon coil appears to be substantially contracted, in agreement with our present perception that PTFE coils are similar to those of polyethylene (PE) or PETFE. There could be subtle differences on the configuration of such polymer coils (PE, PETFE, PTFE) because of size differences between H and F. However, once in their respective solvents at whichever temperatures, the statistical configurations are essentially the same. Finally, we also made a time study on the stability of Teflon solution at 340 °C, as shown in Figure 14. M_w remains constant for over a 24-h period while $\bar{\Gamma}$ ($\theta = 30°$) appears to change after ~10 h. All our measurements were performed immediately after solution preparation within an 8-h period.

In summary, we have developed laser light scattering as a noninvasive analytical technique, especially suitable for intractable polymers such as PPTA (or "Kevlar", a registered trademark of Du Pont), PETFE (or "Tefzel", a registered trademark of Du Pont), and Teflon. With information on M_w and MWD as well as R_g and second virial coefficients, further improvements on polymerization and processing could be considered.

Acknowledgment. B.C. gratefully acknowledges support of this work by the National Science Foundation (Polymers Program, DMR 8617820).

Registry No. PTFE, 9002-84-0.

References and Notes

(1) Chu, B.; Onclin, M.; Ford, J. R. *J. Phys. Chem.* **1984**, *88*, 6566.
(2) Pope, J. W.; Chu, B. *Macromolecules* **1984**, *17*, 2633.
(3) Naoki, M.; Park, I.-H.; Chu, B. *J. Polym. Sci., Polym. Phys. Ed.* **1985**, *23*, 2567.
(4) Chu, B.; Ying, Q.-C.; Wu, C.; Ford, J. R.; Dhadwal, H.; Qian, R.; Bao, J.; Zhang, J.; Xu, C. *Polym. Commun.* **1984**, *25*, 211.
(5) Ying, Q.-C.; Chu, B. *Makromol. Chem., Rapid Commun.* **1984**, *5*, 785.
(6) Chu, B.; Wu, C.; Ford, J. R. *J. Colloid Interface Sci.* **1985**, *105*, 473.
(7) Ying, Q.-C.; Chu, B.; Qian, R.; Bao, J.; Zhang, J.; Xu, C. *Polymer* **1985**, *26*, 1401.
(8) Chu, B.; Ying, Q.-C.; Wu, C.; Ford, J. R.; Dhadwal, H. S. *Polymer* **1985**, *26*, 1408.
(9) Chu, B.; Wu, C. *Macromolecules* **1986**, *19*, 1285.
(10) Chu, B.; Wu, C. *Macromolecules* **1987**, *20*, 93.
(11) Wu, C.; Buck, W.; Chu, B. *Macromolecules* **1987**, *20*, 98.
(12) Chu, B.; Wu, C.; Zuo, J. *Macromolecules* **1987**, *20*, 700.
(13) Chu, B.; Lee, D.-C. *Macromolecules* **1986**, *19*, 1592.
(14) Koppel, D. E. *J. Chem. Phys.* **1972**, *57*, 4814.
(15) Ford, J. R.; Chu, B. In *Proceedings of the 5th International Conference on Photon Correlation Techniques in Fluid Mechanics*; Schulz-DuBois, E. O., Ed.; Springer-Verlag: New York, 1983; pp 303–314.
(16) Chu, B.; Ford, J. R.; Dhadwal, H. S. *Methods Enzymology*; Colowick, S. P., Kaplan, N. O., Eds.; Academic: Orlando, FL, 1985; pp 256–297.
(17) Abbiss, J. B.; Demol, C.; Dhadwal, H. S. *Opt. Acta* **1983**, *30*, 107.
(18) Provencher, S. W. *Biophys. J.* **1976**, *16*, 27; *J. Chem. Phys.* **1976**, *64*, 2772; *Makromol. Chem.* **1979**, *180*, 201.
(19) Version 2, March 1984. Courtesy of S. W. Provencher.

Light Scattering Study of Ionomers in Solution. 2. Low-Angle Scattering from Sulfonated Polystyrene Ionomers

Masanori Hara* and Jhi-Li Wu

Rutgers, The State University of New Jersey, Department of Mechanics and Materials Science, Piscataway, New Jersey 08854. *Received July 20, 1987*

ABSTRACT: Low-angle light scattering studies were conducted for partially sulfonated polystyrene ionomers in a polar and a low-polarity solvent. In the low-polarity solvent tetrahydrofuran (THF), aggregation of ionomers due to the attraction of ion pairs was seen in changes of molecular weight and interaction parameter (second virial coefficient) with ion content. At high ion content, negative interaction parameters were observed. In the polar solvent dimethylformamide (DMF), typical polyelectrolyte behavior was observed in light scattering data. Effective diameters of macroions (ionomers) were used to discuss the effect of counterion and ion content on the structural change of ionomers.

Introduction

Ionomers are a class of ion-containing polymers, which have ionic groups in concentration up to 10–15 mol %, distributed in nonionic backbone chains.[1-3] Since the development of Surlyn resin by Du Pont in 1966,[4] ionomers have caught the attention of people in both industry and academia. This is based on the fact that the incorporation of ions into solid polymers frequently leads to profound changes in properties, such as glass transition temperature and melt viscosity. Consequently, much work has been

0024-9297/88/2221-0402$01.50/0

devoted to elucidating the overall structure-property relationship of ionomers.[1-8] It has been found that the change in properties of ionomers in the solid state is due to the clustering of ion pairs in the medium of low dielectric constant.

Compared with the work on ionomers in solid state, relatively little has been done to investigate the structure-property relationship of ionomers in solution. This is in marked contrast to the situation with regard to another class of ion-containing polymer, polyelectrolytes, where major interest has been concentrated on solution properties.[9-11] Recently, however, the solution properties of ionomers have begun to be studied because of the realization of their unique properties.[12-29]

It has now been widely recognized that ionomers show two types of behavior depending on the polarity of the solvents:[14,27,28] (1) aggregation behavior due to dipolar attractions of ion pairs in nonpolar solvents; (2) polyelectrolyte behavior due to Coulombic interactions between ions in polar solvents.

In nonpolar or low-polarity solvents, ionic groups are not dissociated and form ion pairs, which further coalesce to form ionic aggregates. Therefore, the situation is close to the bulk state of ionomers. Initially, Lundberg et al.[14] showed by viscosity measurements that at low polymer concentration, intramolecular association dominated, while at higher polymer concentration, intermolecular association dominated. Similar results have been obtained for various ionomer systems.[16,24] Although the occurrence of aggregation between ionomer chains in dilute solution has been showed as mentioned, their structure has not been systematically investigated. Recently, Lantman et al.[20,21] and Hara et al.,[26] started to use light scattering technique to elucidate the more detailed structure of ionomers in low-polarity solvents.

In polar solvents, ionic groups are dissociated and cause polyelectrolyte behavior. Again, initially, viscosity measurements[12] were used to show typical polyelectrolyte behavior. Similar studies were conducted for other ionomer systems.[14,16,24] The common point found in these observations is that all ionomers studied in polar solvents showed characteristic polyelectrolyte behavior. Particularly interesting is the fact that even the samples with very low ion content (as low as 0.1 mol %) show polyelectrolyte behavior,[29] although the effect in ionomers is smaller than that in polyelectrolytes in aqueous solutions. More recently, MacKnight et al.[19] reported the broad single peaks in neutron scattering curves, which have been frequently observed for salt-free polyelectrolytes in aqueous solution. Hara et al.[23] reported typical polyelectrolyte behavior in light scattering data from ionomer solutions. Although general polyelectrolyte behavior has been shown to occur for ionomers in polar solvents as mentioned, structural details of their solutions have not been determined.

Here, we use low-angle light scattering to elucidate the structure of ionomers in both polar and nonpolar solvents. This is a second paper in a series of works on the study of ionomer solutions by light scattering. This light scattering technique is one of the direct methods for obtaining information on the structure of macromolecules in solution. This is especially useful in studying the molecular aggregates that are formed due to the attraction between ionic dipoles: since the scattering power is proportional to the square of particle weight, the light scattering method is very sensitive to aggregation behavior.

Experimental Section

Materials. Details concerning the preparation of lightly sulfonated polystyrene and their characterization were described elsewhere.[23,24] Here we use the designation of ionomers proposed by Eisenberg;[2] S-0.032SSA-Na means the copolymer of styrene (S) with sodium styrenesulfonate, whose mole fraction is 0.032. Therefore, ion content in this ionomer is 3.2 mol %. All starting polystyrenes were polystyrene standards (Pressure Chemical) with narrow molecular weight distributions (Table I).

Table I
Ionomer and Polystyrene Samples

mol wt	M_w/M_n	ion content, mol %
400 000	<1.06	0
		0.94
		1.9
9000	<1.06	0
		2.1
		4.0
3500	<1.06	0
		2.0
		5.6

Table II
Specific Refractive Index Increment, dn/dc, of Ionomers and Polystyrenes

mol wt	ion content	dn/dc (THF)	dn/dc (DMF)
400 000	0	0.209	0.162
	0.94	0.193	0.155
	1.9	0.187	0.156
9000	0	0.197	0.158
	2.1	0.177	0.149
	4.0	0.179	0.156
3500	0	0.180	
	2.0	0.175	
	5.6	0.171	

Measurements. Polymer solutions were prepared by dissolving the freeze-dried samples in a proper solvent (DMF, THF) under stirring for a day at room temperature. Light scattering measurements were conducted with a KMX-6 low-angle light scattering photometer (Chromatix) at a wavelength of 633 nm at 25 ± 0.5 °C. This instrument was designed only for measurements at low angles (2–7°) with high precision.[30] The usual calibration was unnecessary, since absolute scattering intensity was directly calculated by geometric parameters and ratio of radiant power.[30,31] Furthermore, the effect of dust (foreign particles) was minimized due to very small scattering volumes (1×10^{-4} cm^3). The effect of large dust particles was easily distinguished by using a flow cell and a recorder. Measurements were carried out at a 6–7° scattering angle, which was small enough to assume that no extrapolation to zero scattering angle was necessary for our systems. The optical clarification of the solution was carried out by passing the solution through two membranes, whose pore sizes were 0.5 and 0.2 (or 0.1) μm, in succession (Fluoropore Filter: Millipore Co, and Nucleopore Filter: Nucleopore Co.). Measurements were done at three different points of the cell window to make sure that the effects of the roughness of the cell windows on scattering were negligible. The specific refractive index increment, dn/dc, was measured at 25 ± 0.1 °C by using a KMX-16 differential refractometer (Chromatix) (Table II).

Light Scattering Equations. Various forms of equations are used for analyzing light scattering data. The most general formula[32] is given by

$$R_\theta = [KcMP(\theta)]\left[1 - \frac{4\pi N}{V}\int_0^\infty \{1 - \rho(r)\}r^2\frac{\sin hr}{hr}\,dr\right] \quad (1)$$

where R_θ is the excess reduced scattered intensity at angle θ from solution. c represents polymer concentration, M (weight-average) molecular weight, and $P(\theta)$ particle scattering factor. N is the number of molecules in the volume V, h is the scattering vector $h = 4\pi n \sin(\theta/2)/\lambda_0$, λ_0 is the wavelength of the light in vacuo, and $\rho(r)$ is the radial distribution function. Since polarized light is used as the incident beam, the optical constant $K = 4\pi^2 n_0^2 (dn/dc)^2/N_0\lambda_0^4$. The first bracket in eq 1 reflects the scattering from a single polymer chain. The second bracket reflects the loss of scattering due to external interference arising from intermo-

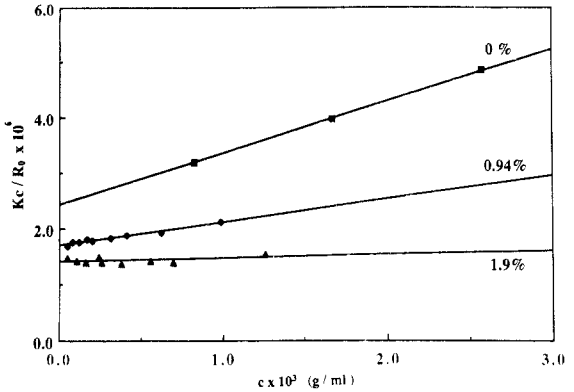

Figure 1. Reciprocal reduced scattered intensity at zero angle, Kc/R_0, against polymer concentration for S-xSSA-Na (M_w 400 000) in THF.

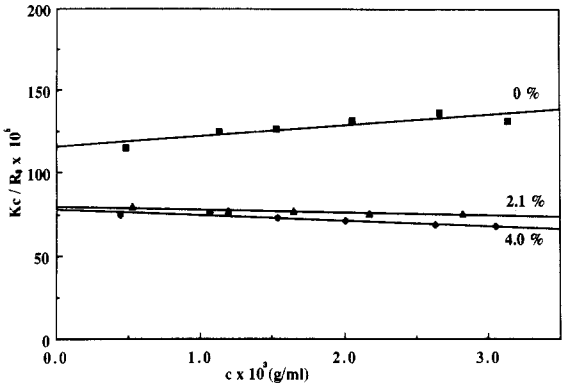

Figure 2. Reciprocal reduced scattered intensity at zero angle, Kc/R_0, against polymer concentration for S-xSSA-Na (M_w 9000) in THF.

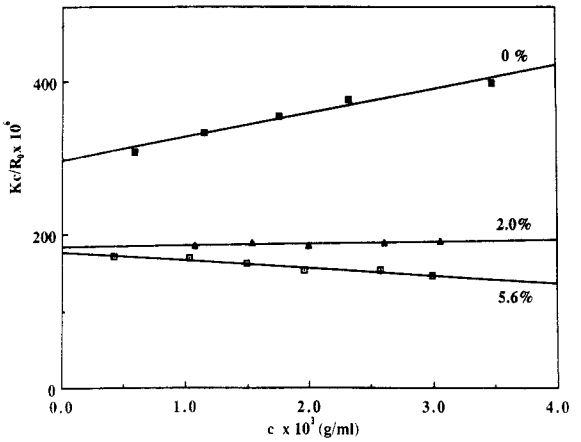

Figure 3. Reciprocal reduced scattered intensity at zero angle, Kc/R_0, against polymer concentration for S-xSSA-Na (M_w 3500) in THF.

lecular interactions, and the integration must be carried out depending on the distribution of particles, i.e., $\rho(r)$.

When the interaction is relatively weak, as is the case of neutral polymers at low concentrations, the interference effect is relatively small and expressed in terms of a virial expasion[33]

$$Kc/R_\theta = 1/MP(\theta) + 2A_2Q(\theta)c + \ldots \quad (2)$$

where $Q(\theta)$ is the interparticle interference factor. This leads to the famous Zimm equation,[34] when $Q(\theta) = 1$. Ionomers in THF will be analyzed by this equation. Since we measure only at very low angles

$$Kc/R_0 = 1/M + 2A_2c + \ldots \quad (3)$$

where $P(0) = 1$ and $Q(0) = 1$.

When the interaction is strong, as is the case of macroions, a virial expansion is not sufficient to describe the interference effect. Doty and Steiner[35] derived equations by considering several interparticle potentials (rigid sphere, electrostatic potential, and Gaussian-type repulsion). It was shown that Kc/R_{90} vs c curves for these three cases were not appreciably different. The simplest model to be utilized is the effective hard sphere model. This model treats the macroions as if they were neutral but have an effective size, which is larger than the real volume because of the long-range repulsive Coulombic interaction. The equation obtained is

$$\frac{Kc}{R_\theta} = \frac{1}{MP(\theta)}\left[1 + \frac{2B'}{M}c\Phi(hD)\right] \quad (4)$$

Here $\Phi(x) = (3/x^3)(\sin x - x\cos x)$ and $B' = (2\pi/3)D^3N_0$; D represents the effective diameter, which is a measure of the range of interactions, and is thought to be a decreasing function of concentration. Ionomers in DMF will be analyzed by this equation. Again, since we use low-angle light scattering

$$\frac{Kc}{R_0} = \frac{1}{M}\left(1 + \frac{4\pi D^3(c)N_0}{3M}c\right) \quad (5)$$

At this time, we do not know the function of $D(c)$. In order to obtain information on macroions, we analyze the initial slope of Kc/R_0 vs c curves. From eq 5

$$\left[\frac{d}{dc}\left(\frac{Kc}{R_0}\right)\right]_{c=0} = \frac{4\pi N_0}{3M^2}D_0^3 \quad (6)$$

D_0 is the effective diameter at zero concentration. This means that from the initial slope of Kc/R_0 vs c curve, we can obtain D_0. Actually, the concept of an effective sphere is equivalent to the concept of an equivalent impenetrable sphere in excluded volume theory for neutral polymers by Flory.[36]

Results and Discussion

Aggregation Behavior. It has been pointed out that ionomer molecules tend to aggregate in nonpolar solvents due to attractions between ionic dipoles (ion pairs).[13,14]

Table III
Weight-Average Molecular Weight, M_w, and Second Virial Coefficient, A_2, for S-xSSA-Na in THF

mol wt	ion content, mol %	M_w	A_2
	0	4.11×10^5	4.7×10^{-4}
400 000	0.94	5.89	2.1
	1.9	7.13	0.23
	0	9.08×10^3	2.9×10^{-3}
9000	2.1	1.25×10^4	−0.92
	4.0	1.28	−1.8
	0	3.51×10^3	2.0×10^{-2}
3500	2.0	5.30	0
	5.6	5.70	−0.51

Figures 1–3 show the reciprocal reduced scattered intensity at zero angle, Kc/R_0, against polymer concentration for ionomers as well as starting PS in THF. In these systems, since a linear relationship is obtained, eq 3 can be used to analyze the data. It is clear that the weight-average molecular weight increases and the second virial coefficient decreases with increasing ion content. These values are summarized in Table III.

Figure 4 shows the change in molecular weight as a function of ion content for the S-xSSA-Na (M_w 9000) sample. First, the molecular weight increases rather sharply and then increases gradually at higher ion content. Other ionomer samples having different molecular weights (400 000 and 3500) show a similar tendency. Figure 5 shows the change in interaction parameter, A_2, as a function of ion content. The A_2 decreases rather sharply, passes the line of $A_2 = 0$ and decreases gradually at higher ion content. Here, we obtain negative A_2 values. This

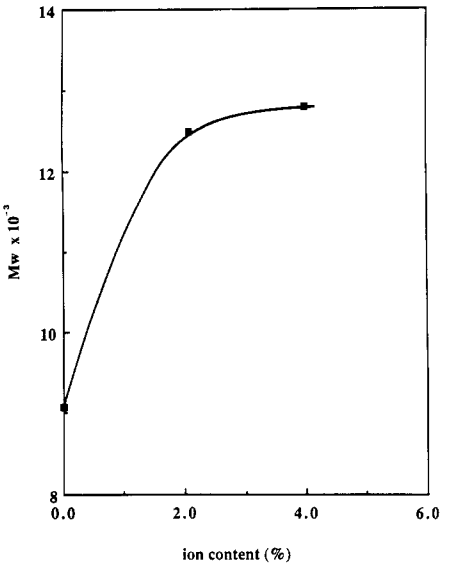

Figure 4. Ion-content dependence of molecular weight of S-xSSA-Na (M_w 9000) in THF.

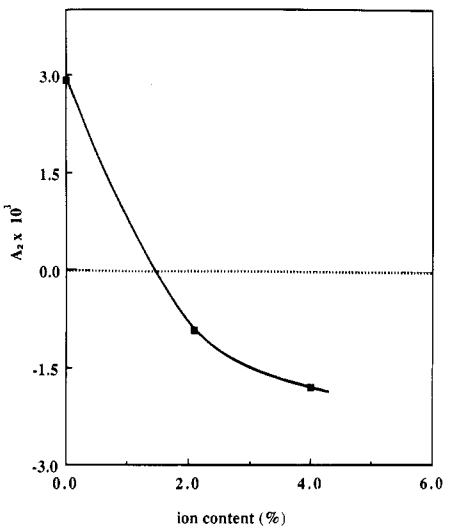

Figure 5. Ion-content dependence of second virial coefficient, A_2, of S-xSSA-Na (M_w 9000).

trend is also similar to other samples having different molecular weight (400 000 and 3500). For the low molecular weight samples, we obtain a transparent solution at even higher ion content than the high molecular weight samples because of the higher solubility.

The decrease in A_2 is attributed to two factors: (1) poor solubility of solvent, since THF is not a good solvent for ionic groups; (2) attraction between ion pairs in low dielectric constant medium. If the former is the only reason, we should obtain the same molecular weight irrespective of the ion content. However, as is shown in Table III and Figure 4, the molecular weight increases with ion content. Therefore, the decrease in A_2 definitely reflects the attractions between ion pairs in THF. These data are consistent with those reported by Lantman et al.[21] and theoretical calculation by Joanny.[37] It was pointed out[37,38] that the second virial coefficient of ionomer solutions is composed of two parts; i.e., $A_2 = A_2' + f^2A_2''$, where A_2 is the overall second virial coefficient, A_2' is the second virial coefficient due to the excluded volume of the backbone chains, A_2'' is the second virial coefficient due to attractions between dipoles (therefore, A_2'' is always negative), and f is ion content. Although, in the original treatment by Joanny,[37] A_2' reflects only the excluded volume of homo-

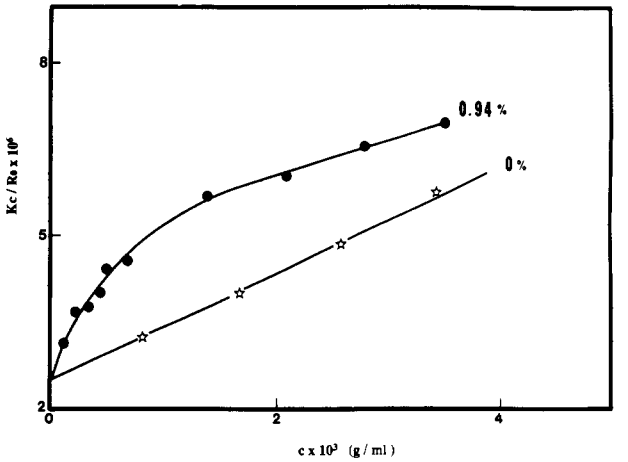

Figure 6. Reciprocal reduced scattered intensity at zero angle, Kc/R_0, against polymer concentration of S-0.0094SSA-Na (M_w 400 000) and PS in DMF.

polymer chains (e.g., polystyrene), it should include the interaction between ionic groups and solvent (i.e., solvent quality); A_2' is actually a decreasing function of ion content. Thus, it is obvious that the overall second virial coefficient, A_2, decreases with increasing ion content, since A_2' decreases and f^2 increases with ion content.

From the above discussion, it is obvious that small molecular aggregates are formed mainly due to attraction between ion pairs. However, it should be pointed out that only a small percentage of ion pairs are participating in the intermolecular association at very dilute concentration. For example, the ionomer whose ion content is 2 mol % and molecular weight is 400 000 has about 80 ion pairs per chain. If one out of 80 ion pairs participates in the intermolecular association, the dimer whose molecular weight is 800 000 can be found. Our experiments shows that the weight-average molecular weight is about 700 000; therefore, the number of ion pairs participating in intermolecular associations at very dilute concentration is only about 1% of the total number of ion pairs.

Polyelectrolyte Behavior. It has been pointed out that ionomers in polar solvents show typical polyelectrolyte behavior.[14,19,23] It is of interest to notice that even ionomers with very low ion content (0.1 mol %) show this behavior.[29] Figure 6 shows the typical Kc/R_0 vs c plot of ionomers:[23] the reciprocal scattered intensity increases sharply from the intercept at zero concentration and bends over at higher concentrations. This behavior was reported for polyelectrolytes (serum albumin[35] and sodium poly(methacrylate)[39]) in aqueous solution, although the reliability of these early measurements are rather poor because of very small scattered intensity from polyelectrolyte/aqueous solution systems and use of less sophisticated instruments at that time. As we pointed out in a previous paper[23] the scattered intensity from ionomers in polar solvents (R_θ = (1–20) × 10^{-6}) is much larger than that from polyelectrolytes in aqueous solution (R_θ = (0.1–1) × 10^{-6}), while the polyelectrolyte behavior was essentially kept. Also, the instrument we use is much more sophisticated with regard to the detection of weak signals. Therefore, it is clear that these curves are characteristic to ionic polymers in polar solvents.

These data are analyzed by using eq 4–6. First, we use eq 6 and obtain effective diameters. One method for obtaining the initial slopes is shown in Figure 7. The slope of each line connected between intercept and each data point in the Kc/R_0 vs c curves are plotted as a function of polymer concentration and are extrapolated to zero concentration. The values obtained by this simple method

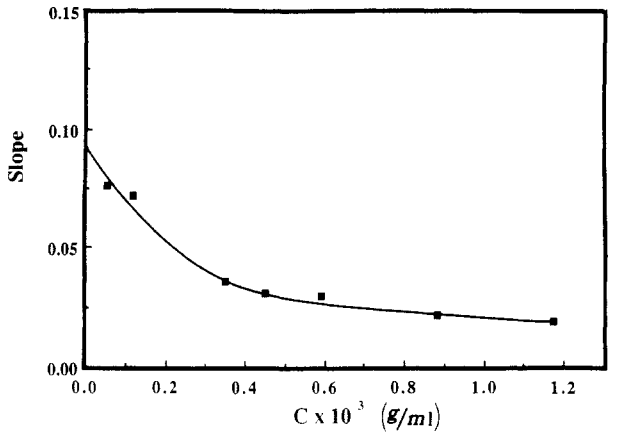

Figure 7. Extrapolation of the slopes to zero concentration for S-0.032SSA-Na (M_w 400 000) in DMF.

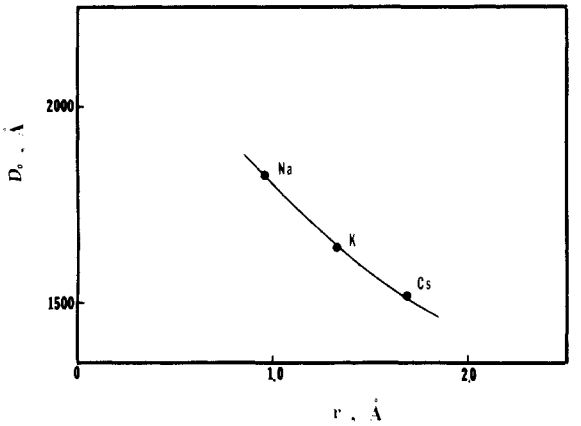

Figure 8. Effective diameter at zero concentration, D_0, against ionic radius of counterion for S-0.032SSA-Na (M_w 400 000) in DMF.

are in good agreement with values obtained by curve fitting using third degree polynomials.[23]

Various effects can now be discussed quantitatively by using the effective diameter; effective diameter reflects the range of intermolecular repulsive interactions. Figure 8 shows the counterion effect on the effective diameters. The original Kc/R_0 vs c curves were reported before.[24] It is clear that the effective diameter decreases with increasing ionic radius of counterion. This is due to the increase in counterion binding with ionic radius for sulfonated ionomer system, which is consistent with previous results.[24] Figure 9 shows the ion content effect. Original Kc/R_0 vs c curves were reported elsewhere.[23] The effective diameter increases linearly with ion content, or effective volume increases with the third power of ion content.

Conclusions

Low-angle light scattering measurements were conducted on partially sulfonated ionomers with sharp molecular weight distributions. Aggregation behavior of ionomers in low-polarity solvent (THF) was discussed more quantitatively in terms of molecular weight and second virial coefficient. It was seen that small aggregates were formed even in very dilute solution. It was reported recently[40] that these aggregates were more time-dependent than originally thought, which is clearly an important subject for further studies. Polyelectrolyte behavior of ionomers in polar solvent (DMF) was discussed in terms of effective diameters of macroions. The effect of ion content and counterion was discussed more quantitatively by using this concept. It is shown that ionomers are a good

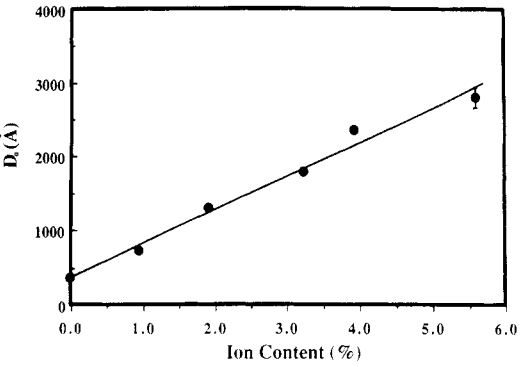

Figure 9. Effective diameter at zero concentration, D_0, against ion content for S-xSSA-Na (M_w 400 000) in DMF. The error bars of data points for samples with less than 4 mol % are within circles.

model system to study characteristic behavior of salt-free polyelectrolytes. Further works by light scattering on this subject will be reported.

Acknowledgment. We thank Drs. J. Scheinbeim and U. P. Strauss for useful discussions. Acknowledgment is also made to the donors of the Petroleum Research Fund, administered by the American Chemical Society, for partial support of this research. This work is also partly supported by NSF (DMR-8513893).

Registry No. DMF, 68-12-2; THF, 109-99-9.

References and Notes

(1) Holliday, L., Ed. *Ionic Polymers*; Applied Science: London, 1975.
(2) Eisenberg, A.; King, M. *Ion*-Containing *Polymers*; Academic: New York, 1977.
(3) MacKnight, W. J.; Earnest, T. R. *J. Polym. Sci., Macromol. Rev.* **1981**, *16*, 41.
(4) Rees, R. W. U.S. Patent 3 264 272, 1966 (assigned to E.I. DuPont de Nemours and Co.).
(5) Bazuin, C. G.; Eisenberg, A. *Ind. Eng. Chem. Prod. Res. Dev.* **1981**, *20*, 271.
(6) MacKnight, W. J.; Lundberg, R. D. *Rub. Chem. Tech.* **1984**, *57*, 652.
(7) Wilson, A. D.; Prosser, H. J., Eds. *Developments in Ionic Polymers*; Applied Science: London, 1983.
(8) Pineri, M.; Eisenberg, A. *Structure and Properties of Ionomers*; D. Reidel: Dordrecht, Holland, 1987.
(9) Rice, S. A.; Nagasawa, M. *Polyelectrolyte Solutions*; Academic: New York, 1961.
(10) Oosawa, F. *Polyelectrolytes*; Marcel Dekker: New York, 1971.
(11) Selegny, E., Ed. *Polyelectrolytes*; D. Reidel: Dordrecht, Holland, 1974.
(12) Rochas, C.; Domard, A.; Rinaudo, M. *Polymer* **1979**, *20*, 1979.
(13) Lundberg, R. D.; Makowski, H. S. *J. Polym. Sci., Polym. Phys. Ed.* **1980**, *18*, 1821.
(14) Lundberg, R. D.; Phillips, R. R. *J. Polym. Sci., Polym. Phys. Ed.* **1982**, *20*, 1143.
(15) Broze, G.; Jérôme, R.; Teyssié, Ph. *Macromolecules* **1981**, *14*, 224; **1982**, *15*, 920; **1982**, *15*, 1300.
(16) Niezette, J.; Vanderschueren, J.; Aras, L. *J. Polym. Sci., Polym. Phys. Ed.* **1984**, *22*, 1845.
(17) Tant, M. R.; Wilkes, G. L.; Storey, R. F.; Kennedy, J. P. *Polym. Prepr. (Am. Chem. Soc., Div. Polym. Chem.)* **1984**, *25*, 118.
(18) Fitzgerald, J. J.; Weiss, R. A. *ACS. Symp. Ser.* **1986**, *No. 302*, 35.
(19) MacKnight, W. J.; Lantman, C. W.; Lundberg, R. D.; Sinha, S. K.; Peiffer, D. G. *Polym. Prepr. (Am. Chem. Soc., Div. Polym. Chem.)* **1986**, *27*(1), 327.
(20) Lantman, C. W.; MacKnight, W. J.; Lundberg, R. D.; Peiffer, D. G.; Sinha, S. K., *Polym. Prepr. (Am. Chem. Soc., Div. Polym. Chem.)* **1986**, *27*(2), 292.
(21) Lantman, C. W.; MacKnight, W. J.; Peiffer, D. G.; Sinha, S. K.; Lundberg, R. D. *Macromolecules* **1987**, *20*, 1096.
(22) Aldebert, P.; Dreyfus, B.; Pineri, M. *Macromolecules* **1986**, *19*, 2651.

(23) Hara, M.; Wu, J. *Macromolecules* **1986**, *19*, 2887.
(24) Hara, M.; Lee, A. H.; Wu, J. *J. Polym. Sci., Polym. Phys. Ed.* **1987**, *25*, 1407.
(25) Hara, M.; Lee, A. H.; Wu. J. *Polym. Prepr. (Am. Chem. Soc., Div. Polym. Chem.)* **1985**, *26*(2), 257; **1986**, *27*(1), 335; **1986**, *27*(2), 177.
(26) Hara, M.; Lee, A. H.; Wu, J. *Polym. Prepr. (Am. Chem. Soc., Div. Polym. Chem.)* **1987**, *28*(1), 198.
(27) Marina, M. G.; Monakov, Y. B.; Rafikov, S. R. *Uspekhi Khim* **1979**, *48*, 722; *Russ. Chem. Rev.* **1979**, *48*, 389.
(28) Shade, H.; Gartner, K. *Plaste Kautschuk* **1974**, *21*, 825.
(29) Hara, M.; Wu, J.; Lee, A. H., unpublished work.
(30) Kaye, W.; Havlik, A. J. *Appl. Opt.* **1973**, *12*, 541.
(31) *Chromatix KMX-6 Low Angle Light Scattering Photometer Instruction Manual*
(32) Zernicke, F.; Prins, J. A. *Z. Phys.* **1927**, *41*, 184.
(33) Flory, P. J.; Bueche, A. M. *J. Polym. Sci.* **1958**, *27*, 219.
(34) Zimm, B. H. *J. Chem. Phys.* **1948**, *16*, 1093; **1948**, *16*, 1099.
(35) Doty, P.; Steiner, R. F. *J. Chem. Phys.* **1952**, *20*, 85.
(36) Flory, P. J. *Principles of Polymer Chemistry*; Cornell University Press: Ithaca, NY, 1953.
(37) Joanny, J. F. *Polymer* **1980**, *21*, 71.
(38) Cates, M. E.; Witten, T. A. *Macromolecules* **1986**, *19*, 732.
(39) Oth, A.; Doty, P. *J. Phys. Chem.* **1952**, *56*, 43.
(40) Peiffer, D. G.; Kaladas, J.; Duvdevani, I.; Higgins, J. S. *Macromolecules* **1987**, *20*, 1397.

Morphology Control of Binary Polymer Mixtures by Spinodal Decomposition and Crystallization. 2. Further Studies on Polypropylene and Ethylene–Propylene Random Copolymer†

Nobuyuki Inaba, Takeshi Yamada, and Shyunichi Suzuki

Polymer Research Laboratory, Idemitsu Petrochemical Co. Ltd., Anegasaki, Ichihara City, Chiba, 299-01, Japan

Takeji Hashimoto*

Department of Polymer Chemistry, Kyoto University, Kyoto 606, Japan.
Received April 21, 1987; Revised Manuscript Received August 17, 1987

ABSTRACT: Morphology control of binary polymer mixtures through spinodal decomposition and crystallization was studied by using polypropylene and ethylene–propylene random copolymer as a model system. The solid texture consisted of dual morphological units, (i) the modulated network structure resulting from spinodal decomposition and its coarsening processes in the isothermal demixing of the mixture in the molten liquid state and (ii) the spherulite structure resulting from crystallization by subsequent cooling of the demixing liquid. Interrelations of the two morphological units in the solid texture were closely investigated by polarized and phase-contrast optical microscopy and light scattering by changing isothermal demixing conditions and crystallization conditions. A criterion for conservation of the modulated structure developed in the demixing liquid during and after the crystallization is discussed, and the locking-in phenomenon of the demixing processes by crystallization is clearly presented in some certain cases and was found to be responsible for the conservation of the structure existing in the liquid. Some unique morphologies are presented schematically in the text.

I. Introduction

In a previous paper[1] we proposed a particular method of morphology control for polymer mixtures such as isotactic polypropylene (PP) and ethylene–propylene random copolymer (EPR), which can be immiscible in the molten liquid state and contain a crystallizable component, at least as one component. The method involves liquid–liquid (L–L) phase separation to a certain demixed state by spinodal decomposition, subsequent coarsening processes in the molten liquid state, and then crystallization by cooling the demixing liquid mixture. It was found[1] that a unique demixed structure in the molten liquid state, i.e., the *modulated*, bincontinous, and periodic structure,[2] is conserved during the rapid crystallization process, resulting in space-filling PP spherulites of average radius R within which the L–L demixing structure of the spacing Λ_m ($\Lambda_m < R$) is conserved, as a particular example (this phenomenon being designated as "memory conservation").

In this paper we further investigate the interrelation between the two morphological units, i.e., the *modulated structure* and the *spherulites*, in the solid texture by changing further demixing and crystallization conditions. The interrelation will be fully investigated by polarized and phase-contrast light microscopy and by light scattering. We explore the cases where $R < \Lambda_m$ as well as $R > \Lambda_m$ as in the previous case[1] by changing the time spent for demixing in the molten liquid state before crystallization.

We will explore slow isothermal crystallization as compared with a rapid crystallization involved in athermal quenching (one of the "diffusion-limited" crystallization[1] conditions) as in the previous case in order to investigate criteria in which the "structure memory" of the L–L demixing is conserved during the crystallization process. The criterion will be studied both by optical microscopy and by studying crystallization kinetics. The rapid crystallization which is found to meet the criterion involves "the diffusion-limited crystallization",[1] i.e., the crystallization occurring in and through PP-rich domains and by finding and following PP-rich domains without invoking long-range rearrangement of PP molecules such as segregation of the EPR component from crystallization front of PP and destruction of the modulated structure developed before crystallization. It will be shown also that the crystallization is very effective to *lock-in* further growth of the L–L demixing.

II. Experimental Methods

The details of the experimental methods were described in the previous paper.[1] Here we briefly describe only the essential part.

† Presented in part at the 34th Polymer Symposium, the Society of Polymer Science, Japan, Sept 26–28, 1985. Inaba, N.; Sato, K.; Suzuki, S.; Hashimoto, T. *Polym. Prepr. Jpn., Soc. Polym. Sci., Jpn.* **1985**, *34*, 2809.

0024-9297/88/2221-0407$01.50/0